

Observation of an extended magnetic field penetration in amorphous superconducting MoGe films

Taichiro Nishio,^{1,*} Satoru Okayasu,¹ Jun-ichi Suzuki,¹ Nobuhito Kokubo,² and Kazuo Kadowaki³

¹ASRC, Japan Atomic Energy Agency, Tokai, Ibaraki 319-1195, Japan

²Center for Research and Advancement in Higher Education, Kyushu University, Fukuoka 810-0044, Japan

³Institute of Materials Science, University of Tsukuba, Tsukuba, Ibaraki 305-8573, Japan

(Received 28 June 2007; revised manuscript received 19 October 2007; published 11 February 2008)

We have observed the magnetic field distribution of a vortex generated in amorphous (α)-MoGe thin films with various thicknesses (d) ($d < \lambda$, where λ is the penetration depth) with a scanning superconducting quantum interference device microscope. From the analyses of the field distribution as functions of film thickness and temperature, it is found that an effective in-plane penetration depth (Λ) extends with decreasing d , in accordance with the Pearl prediction $\Lambda = 2\lambda^2/d$. Temperature dependence of Λ is also consistent with the two-fluid model involving the Pearl prediction.

DOI: [10.1103/PhysRevB.77.052503](https://doi.org/10.1103/PhysRevB.77.052503)

PACS number(s): 74.78.Db, 74.81.Bd, 85.25.Dq

Pearl¹ calculated, in 1964, the distribution of the supercurrent density around a vortex core in an infinitesimally thin superconducting film [$d \ll \lambda$, where d and λ are a film thickness and the penetration depth, respectively, i.e., a two dimensional (2D) superconductor] using the London model. The result shows that the radial dependence of the current density changes from $1/r$ to $1/r^2$ at $r \sim \Lambda$ ($=2\lambda^2/d$), while it changes from $1/r$ to exponential cutoff at $r \sim \lambda$ in a bulk superconductor. This indicates that the in-plane penetration depth actually corresponds to Λ rather than λ in a 2D superconductor, and furthermore, an interaction between vortices in a 2D superconductor becomes logarithmic over a longer range $r < \Lambda$ than $r < \lambda$ in a bulk superconductor, so that the properties of vortex in a 2D superconductor differ from those of Abrikosov vortex in a bulk superconductor. This vortex with a long-range interaction (the so-called Pearl vortex) has been intensively investigated in terms of a symmetry of the 2D Coulomb gas,²⁻⁶ on the other hand, experimental confirmation of the extension in penetration depth has not been made with sufficient quality until experimental tools have been developed.

Recent developments in scanning superconducting quantum interference device (SQUID) microscopy have made it possible to directly estimate the penetration depth of a micrometer size. Just recently, Tafuri *et al.*⁷ have given the first magnetic images of vortices in artificial cuprate films (2D superconductors) by a scanning SQUID microscope (SSM) technique. They show that Λ can be estimated by fitting the anisotropic London model⁸⁻¹⁰ to the magnetic field distribution of a vortex derived from the vortex images. However, they have found that there was much difference between the in-plane penetration depth λ_{ab} inferred from observed Λ and that in bulk cuprates with comparable critical temperatures. Therefore, it is necessary to confirm the agreement between Λ derived by scanning SQUID microscopy and the Pearl prediction by using a simple system such as a conventional superconductor.

In this Brief Report, we present direct observation of the magnetic field distribution of vortices in superconducting amorphous (α)-MoGe thin films with variable thicknesses from the bulk region ($d \sim \lambda$) to the ultrathin film region

($d \ll \lambda$) with a SSM. A film thickness was systematically changed over a range from 30 to 400 nm where corresponding Λ is expected to be above several micrometers. In this length scale, it is valid to determine Λ from the magnetic field distribution measured by a SSM technique. The Λ values are derived from the vortex images by using the numerical fitting of the field distribution of a vortex obtained from the anisotropic London model. Thickness dependence and temperature dependence of Λ were investigated as shown below.

Thin films of α -MoGe with thicknesses of 30, 55, 100, 200, and 400 nm were sputtered on water-cooled Si substrates in a magnetron rf sputtering system, then the α -MoGe films were covered with 100 nm thick SiO₂ layers to protect the α -MoGe films from scratching by a cantilever on which a SQUID sensor was equipped. Thicknesses of the films were estimated by the sputtering time and the deposition rate, which was calibrated by profilometric measurements of films prepared under identical deposition conditions. We estimate that the accuracy of the determinations is within 10%. Transport measurements show that the superconducting transition temperature T_c and normal state resistivity of all films are 5.7 K and 1.56 $\mu\Omega$ m, respectively. The penetration depths $\lambda(0)$ were estimated to be 550 nm from the standard expression¹¹ in the dirty limit.

Magnetic images of vortices were obtained by using a prototype SSM (SQM-2000, SII NanoTechnology, Inc.).^{12,13} A SQUID sensor consists of a Nb pickup loop and a SQUID magnetometer. The circular Nb SQUID pickup loop with an inner diameter of 8 μm , which was newly designed to eliminate an extrinsic effect (the so-called tail effect) due to the nonideal geometry of the pickup loop, scans the surface of superconductors, keeping a distance of 4–5 μm between the surface and the pickup loop. The distance can be estimated by fitting monopole approximation¹⁴ to the field distribution of a vortex from a SSM image in a thick superconducting film. A magnetic flux resolution of the SQUID magnetometer is better than 5 $\mu\phi_0/\text{Hz}^{1/2}$, where $\phi_0 (=2.07 \times 10^{-15} \text{ T m})$ is the flux quantum. That corresponds to a field noise of $\sim 10^{-10} \text{ T/Hz}^{1/2}$ referred to the pickup loop. A spatial resolution is limited to $\sim 2.5 \mu\text{m}$.¹³ The films were field cooled to the lower temperatures than T_c .

We numerically calculate the field distribution of a vortex above the sample surface using the following anisotropic London model.⁸⁻¹⁰ We consider that a superconducting thin film is situated at $z=0$. Since $\text{rot } \mathbf{h} = \text{div } \mathbf{h} = 0$ outside the superconductor, a scalar potential ψ can be introduced for the magnetic field outside the thin film,

$$\mathbf{h} = \nabla \psi, \quad \nabla^2 \psi = 0. \quad (1)$$

A general solution of Eq. (1) at $z=0$ which vanishes at $z \rightarrow \infty$ in the empty upper half-space is given by the following equation:

$$\psi(\mathbf{r}, z) = \int \frac{d^2 \mathbf{k}}{(2\pi)^2} \psi(\mathbf{k}) e^{i\mathbf{k}\mathbf{r} - kz}, \quad (2)$$

where $\mathbf{k} = (k_x, k_y)$, $\mathbf{r} = (x, y)$, and $k = |\mathbf{k}|$. Here, $\psi(\mathbf{k})$ is 2D Fourier transform of $\psi(\mathbf{r}, z=0)$. According to Kogan,⁹ $\psi(\mathbf{k})$ can be written as

$$\psi(\mathbf{k}) = -\frac{\phi_0}{k(1+k\Lambda)}, \quad (3)$$

including Λ introduced by Pearl,¹ since $h_z(\mathbf{k}) = -k\psi(\mathbf{k})$ for the upper half-space. The distribution of the potential $\psi(\mathbf{r}, z)$ outside the superconductor follows from Eqs. (2) and (3),

$$\psi(\mathbf{r}, z) = -\frac{\phi_0}{2\pi} \int_0^\infty \frac{e^{-kz} dk J_0(kr)}{1+k\Lambda}, \quad (4)$$

where J_0 is the Bessel function. Using an equation $\frac{1}{1+k\Lambda} = \int_0^\infty ds e^{-(1+k\Lambda)s}$, we obtain

$$\psi(\mathbf{r}, z) = -\frac{\phi_0}{2\pi} \int_0^\infty dk \int_0^\infty ds e^{-kz - (1+k\Lambda)s} J_0(kr) \quad (5a)$$

$$= -\frac{\phi_0}{2\pi} \int_0^\infty ds \frac{e^{-s}}{\sqrt{r^2 + (z+s\Lambda)^2}}, \quad (5b)$$

where we use an equation 11.4.39 in a mathematical table.¹⁵ Finally, the field distribution outside the superconductor in real space is given by setting this equation into Eq. (1). If $z \gg \Lambda$, the solution approaches to monopole approximation, becoming independent of Λ . However, since we expect $z \leq \Lambda$ in our case, we can fit the numerical calculations resulted from these equations involving two parameters of z and Λ . In our measurement, the pickup loop probes the magnetic flux passing through the loop and the output is the average magnetic flux density in the loop area, so that the fitting procedures include convolution with the size of the pickup loop: our London model is simply integrated over the probe area and divided by the area to take account of convolution of the field over the pickup loop.

Figures 1(a) and 1(b) show magnetic images of vortices in α -MoGe films with thicknesses of 400 and 100 nm at an applied field of 10 μT at 4.5 K, respectively. Despite such a low applied field, the long-range lattice order with the intervortex distance of about 15 μm is observed in the 400 nm thick film, while a disordered vortex arrangement is found in the 100 nm thick film. The presence of the lattice order suggests that our α -MoGe films are simply of high quality.

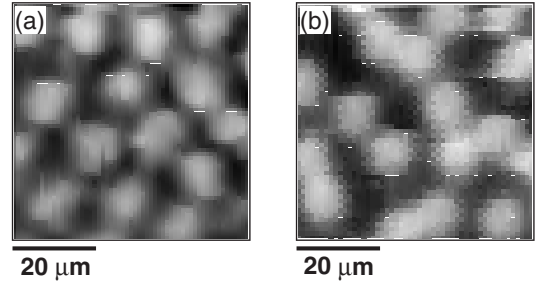


FIG. 1. (a) Magnetic images of vortices forming triangular lattice in the 400 nm thick α -MoGe film and (b) a disordered vortex arrangement in the 100 nm thick film at an applied magnetic field of 10 μT perpendicular to the film surface at 4.5 K. The shade corresponds to a range of the magnetic flux density from 0 to 10 μT .

The observation of the disordered structure of the vortex arrangement in the 100 nm thick film can be explained by the collective pinning theory,^{16,17} where the pinning force per unit volume increases with decrease in film thickness. The increase of the pinning force makes the elasticity between vortices lower and makes it more favorable that vortices are individually trapped by pinning centers than vortices form the Abrikosov lattice. Therefore, dislocations in vortex lattices come to be induced with decreasing thickness.

Figures 2(a) and 2(b) show vortex images in α -MoGe films with thicknesses of 400 and 30 nm taken at an applied field of 1 μT at 4.5 K, respectively. The observed peak magnetic flux density at the center of the vortex in Fig. 2(b) is approximately ten times lower than that in Fig. 2(a) (the diminishing of the peak magnetic flux density with decreasing thickness makes it hard to observe a vortex in films with thicknesses less than 30 nm) and the vortex image in Fig. 2(b) seems to be somewhat larger than that in Fig. 2(a). As shown in Figs. 2(c) and 2(d), the full widths at half maxi-

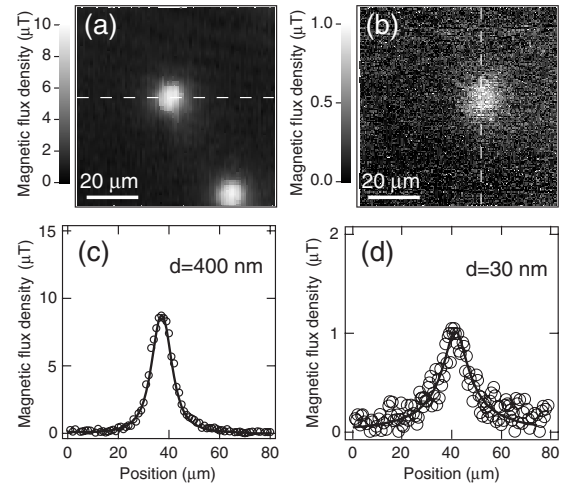


FIG. 2. Magnetic images of vortices in the α -MoGe films with thicknesses of (a) 400 nm and (b) 30 nm at a perpendicular magnetic field of 1 μT at 4.5 K, respectively. [(c) and (d)] The magnetic field profiles of the vortices along the dashed lines in (a) and (b), respectively. The solid lines shown in (c) and (d) are the fits of numerical calculations (see text).

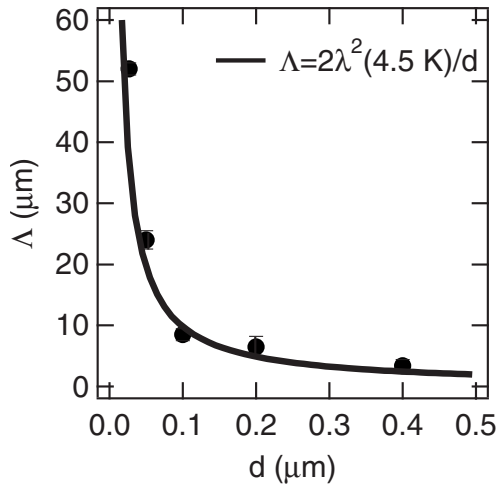


FIG. 3. Thickness dependence of Λ at 4.5 K in comparison with the Pearl relation $\Lambda=2\lambda^2/d$, which is shown by a solid line (see text). The error bars are assigned by a doubling of the χ^2 values of the fits.

imum of the vortex images are 10 and 18 μm for $d=400$ nm and $d=30$ nm, respectively. These widths, however, do not necessarily mean the penetration depth of the samples because the flux lines associated with a vortex extend out of the surface of the film and the flux probed by the SQUID pickup loop is a few micrometers away from the surface of the superconductor. In order to obtain the correct value for Λ , it is necessary to make appropriate numerical calculations from Eqs. (1)–(4), (5a), and (5b).

As a result of the fitting, we obtain $z=4.0$ μm and $\Lambda=3.9$ μm for the 400 nm thick film and $z=4.8$ μm and $\Lambda=52$ μm for the 30 nm thick film, where z is the distance between the pickup loop and the surface of the superconductor. The z values are consistent with those determined by fitting monopole approximation¹⁴ to a vortex image in a 200 nm thick Nb film [$\lambda\sim 50$ nm (Ref. 18)]. The Λ values are indeed larger than λ of 670 nm measured with a two-coil screening technique¹⁹ at 4.2 K and strongly depend on the peak magnetic flux density, which makes it possible to determine Λ by the fitting: the SQUID magnetometer can distinguish a slight variation of the magnetic flux density with an increase of Λ . A similar feature has also been pointed out by Tafuri *et al.*⁷

Figure 3 shows the thickness dependence of Λ derived by the fitting of the data for five different films with thicknesses of 30, 55, 100, 200, and 400 nm at 4.5 K in comparison with the Pearl relation $\Lambda=2\lambda^2/d$. Assuming that temperature dependence of λ follows two-fluid relation²⁰ $\lambda(T)=\lambda(0)[1-(T/T_c)^4]^{-1/2}$ in this superconductor, where $\lambda(0)$ and T_c are 550 nm and 5.7 K obtained from our transport measurement, respectively, we derive a theoretical Λ curve at 4.5 K from the relation $2\lambda^2(T)/d$ denoted by a solid line. As shown in Fig. 3, all the experimental points fall onto the solid curve predicted by Pearl¹ on the assumption of the two-fluid model within experimental errors.

In order to elucidate temperature dependence of Λ , we have also taken vortex images at various temperatures for the

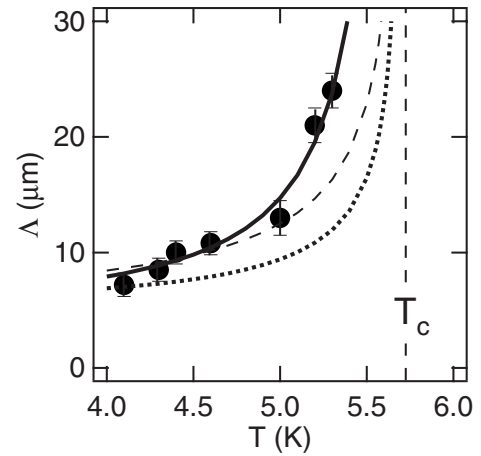


FIG. 4. Temperature dependence of Λ for the 100 nm thick film is compared with theoretical expressions. The filled circles represent experimental data. The dotted and the broken curves show dependencies $\Lambda(0)[1-(T/T_c)^4]^{-1/2}$ and $\Lambda(0)[1-(T/T_c)^2]^{-1/2}$, respectively, where $\lambda(0)=550$ nm and $T_c=5.7$ K. The solid curve represents the result obtained from Eq. (6) (see text). The error bars are assigned the same as Fig. 3.

100 nm thick film. Figure 4 shows the temperature dependence of Λ obtained for a temperature range from 4.1 to 5.3 K. The Λ value corresponds to the screening length λ_{scr} in a 2D superconductor, and as a film thickness increases, λ_{scr} continuously becomes closer to λ_{scr} in bulk superconductors: λ , which is expected to have a temperature dependence close to $\propto[1-(T/T_c)^4]^{-1/2}$.²⁰ In order to check that there is difference in the temperature dependence of λ_{scr} between the 100 nm thick film and bulk superconductors, first, the observed dependence of λ_{scr} is compared with that in the bulk region in Fig. 4. As a result, it seems that the observed dependence is completely different from the dependence $\propto[1-(T/T_c)^4]^{-1/2}$: $\Lambda(0)[1-(T/T_c)^4]^{-1/2}$ with experimental values $\lambda(0)=550$ nm and $T_c=5.7$ K. A temperature dependence closer to $\propto[1-(T/T_c)^2]^{-1/2}$ has indeed been observed in a superconducting film $\text{YBa}_2\text{Cu}_3\text{O}_{7-\delta}$.²¹ In case of weak-coupling superconductors, a microscopic theory²⁰ also gives a temperature dependence $\propto[1-(T/T_c)^2]^{-1/2}$. Taking account of these results, we also compare the experimental results with a dependence $\propto[1-(T/T_c)^2]^{-1/2}$: $\Lambda(0)[1-(T/T_c)^2]^{-1/2}$. The experimental points fall onto a curve $\Lambda(0)[1-(T/T_c)^2]^{-1/2}$ in the lower temperature region in Fig. 4 while it deviates clearly in the higher temperature region. Those suggest that obviously the temperature dependence of λ_{scr} in the 100 nm thick film differs from that in the bulk region and this film lies deeply in the Pearl vortex regime.

We reconsider the theoretical estimation of the thickness dependence of Λ at 4.5 K in Fig. 3. On the basis of the two-fluid model, we assume that temperature dependence of λ follows the relation $\lambda(0)[1-(T/T_c)^4]^{-1/2}$. As far as we know, there has been no systematic measurement of temperature dependence of λ for α -MoGe films. However, a measurement of λ by Plourde *et al.*¹⁹ agrees with the expectation at 4.2 K for the two-fluid model, which is favorable to the two-fluid model. From two-fluid dependent $\lambda(T)$ and the Pearl relation $2\lambda^2(T)/d$, we obtain

$$\Lambda(T) = \frac{\Lambda(0)}{1 - (T/T_c)^4}. \quad (6)$$

If $\lambda(0)$ and T_c are 550 nm and 5.7 K, respectively, this equation gives the curve denoted by a solid line in Fig. 4. As a result of the comparison, the experimental points fall onto the curve from Eq. (6) within experimental errors. The fact strongly supports that the experimental thickness dependence at 4.5 K is consistent with the prediction at 4.5 K derived from Eq. (6), as shown in Fig. 3.

In conclusion, the vortex images for 2D superconductors have been studied systematically with various film thicknesses from 30 to 400 nm. From numerical analysis for the cross section of the magnetic field distribution of a vortex,

the effective in-plane penetration depth Λ has been determined. As a result, thickness dependence of Λ obeys the Pearl prediction $2\lambda^2/d$. It is also found that temperature dependence of Λ follows Eq. (6) derived by two-fluid relation and $2\lambda^2/d$.

We thank P. H. Kes, M. Machida, and Y. Mawatari for useful discussions and T. Nishizaki for his help in patterning of films for transport measurement. This work has partly been supported by the Strategic Research Networks “Nanoscience and Engineering in Superconductivity,” JSPS core-to-core program, and the 21st century COE program in the graduate school of pure and applied sciences in University of Tsukuba and the Ministry of Education, Culture, Sports, Science and Technology of Japan.

*Present address: INPAC-Institute for Nanoscale Physics and Chemistry, Katholieke Universiteit Leuven, Celestijnenlaan 200D, B-3001 Leuven, Belgium. taichiro.nishio@fys.kuleuven.be

¹J. Pearl, Appl. Phys. Lett. **5**, 65 (1964).

²V. L. Berezinskii, Zh. Eksp. Teor. Fiz. **61**, 1144 (1974) [Sov. Phys. JETP **34**, 610 (1972)].

³J. M. Kosterlitz and D. J. Thouless, J. Phys. C **6**, 1181 (1973).

⁴M. R. Beasley, J. E. Mooij, and T. P. Orlando, Phys. Rev. Lett. **42**, 1165 (1979).

⁵P. Minnhagen, Rev. Mod. Phys. **59**, 1001 (1987).

⁶V. G. Kogan, Phys. Rev. B **75**, 064514 (2007).

⁷F. Tafuri, J. R. Kirtley, P. G. Medaglia, P. Orgiani, and G. Balmistrino, Phys. Rev. Lett. **92**, 157006 (2004).

⁸V. G. Kogan, A. Yu. Simonov, and M. Ledvij, Phys. Rev. B **48**, 392 (1993).

⁹V. G. Kogan, Phys. Rev. B **49**, 15874 (1994).

¹⁰V. G. Kogan, V. V. Dobrovitski, J. R. Clem, Y. Mawatari, and R. G. Mints, Phys. Rev. B **63**, 144501 (2001).

¹¹P. H. Kes and C. C. Tsuei, Phys. Rev. B **28**, 5126 (1983).

¹²K. Chinone, S. Nakayama, T. Morooka, A. Odawara, and M.

Ikeda, IEEE Trans. Appl. Supercond. **7**, 3271 (1997).

¹³T. Morooka, S. Nakayama, A. Odawara, M. Ikeda, S. Tanaka, and K. Chinone, IEEE Trans. Appl. Supercond. **9**, 3491 (1999).

¹⁴A. M. Chang, H. D. Hallen, L. Harriott, H. F. Hess, H. L. Kao, J. Kwo, R. E. Miller, R. Wolfe, J. van der Ziel, and T. Y. Chang, Appl. Phys. Lett. **61**, 1974 (1992).

¹⁵*Handbook of Mathematical Functions*, edited by M. Abramowitz and A. Stegun (Wiley, New York, 1972).

¹⁶A. I. Larkin and Yu. N. Ovchinnikov, J. Low Temp. Phys. **34**, 409 (1979).

¹⁷P. H. Kes and C. C. Tsuei, Phys. Rev. Lett. **47**, 1930 (1981).

¹⁸S.-W. Han, J. Farmer, H. Kaiser, P. F. Miceli, I. V. Roshchin, and L. H. Greene, Phys. Rev. B **62**, 9784 (2000).

¹⁹B. L. T. Plourde, D. J. Van Harlingen, N. Saha, R. Besseling, M. B. S. Hesselberth, and P. H. Kes, Phys. Rev. B **66**, 054529 (2002).

²⁰M. Tinkham, *Introduction to Superconductivity*, 2nd ed. (McGraw-Hill, New York, 1996).

²¹S. M. Anlage, B. W. Langley, G. Deutscher, J. Halbritter, and M. R. Beasley, Phys. Rev. B **44**, 9764 (1991).